Factors affecting nitrate distribution in shallow groundwater under a beef farm in South Eastern Ireland

O. Fenton [a,*], K.G. Richards [a], L. Kirwan [a,b], M.I. Khalil [a], M.G. Healy [c]

[a] Teagasc, Johnstown Castle, Environmental Research Centre, Co. Wexford, Rep. of Ireland
[b] Waterford Institute of Technology, Co. Waterford, Rep. of Ireland
[c] Department of Civil Engineering, National University of Ireland, Galway, Rep. of Ireland

ARTICLE INFO

ABSTRACT

Groundwater contamination was characterised using a methodology which combines shallow groundwater geochemistry data from 17 piezometers over a 2 yr period in a statistical framework and hydrogeological techniques. Nitrate–N (NO_3-N) contaminant mass flux was calculated across three control planes (rows of piezometers) in six isolated plots. Results showed natural attenuation occurs on site although the method does not directly differentiate between dilution and denitrification. It was further investigated whether NO_3-N concentration in shallow groundwater (<5 m below ground level) generated from an agricultural point source on a 4.2 ha site on a beef farm in SE Ireland could be predicted from saturated hydraulic conductivity (K_{sat}) measurements, ground elevation (m Above Ordnance Datum), elevation of groundwater sampling (screen opening interval) (m AOD) and distance from a dirty water point pollution source. Tobit regression, using a background concentration threshold of 2.6 mg NO_3-N L^{-1} showed, when assessed individually in a step wise procedure, K_{sat} was significantly related to groundwater NO_3-N concentration. Distance of the point dirty water pollution source becomes significant when included with K_{sat} in the model. The model relationships show areas with higher K_{sat} values have less time for denitrification to occur, whereas lower K_{sat} values allow denitrification to occur. Areas with higher permeability transport greater NO_3-N fluxes to ground and surface waters. When the distribution of Cl^- was examined by the model, K_{sat} and ground elevation had the most explanatory power but K_{sat} was not significant pointing to dilution having an effect. Areas with low NO_3 concentration and unaffected Cl^- concentration points to denitrification, low NO_3 concentration and low Cl^- chloride concentration points to dilution and combining these findings allows areas of denitrification and dilution to be inferred. The effect of denitrification is further supported as mean groundwater NO_3-N was significantly ($P < 0.05$) related to groundwater N_2/Ar ratio, redox potential (Eh), dissolved O_2 and N_2 and was close to being significant with N_2O ($P = 0.08$). Calculating contaminant mass flux across more than one control plane is a useful tool to monitor natural attenuation. This tool allows the identification of hot spot areas where intervention other than natural attenuation may be needed to protect receptors.

© 2009 Elsevier Ltd. All rights reserved.

1. Introduction

Delineation of an elevated nitrate (NO_3-N) plume in shallow groundwater is difficult as NO_3-N concentration differences may be prevalent over short distances. As a result of high denitrification capacity, NO_3-N concentration may be low at the centroid of the plume. Contaminated groundwater in aquifers with low hydraulic conductivity (K_{sat}) may represent a long-term threat to groundwater due to long travel times from source to receptor. A shallow watertable allows reduction of nitrate through denitrification before recharge reaches deeper groundwater (Boland and Buijze, 2002). The thickness and permeability of subsoil can control groundwater vulnerability (Lee, 1999). In such shallow groundwater sites reduction of NO_3-N through denitrification may provide the basis for remediation. Monitored natural attenuation is a valid method in sites with low permeability and high denitrification capacity, leading to a low vulnerability status. In such scenarios surface water and not deeper groundwater may be a potential receptor for NO_3-N pollution.

In spite of efficient nutrient management practices, agricultural activities, such as application methods and storage, are probably

* Corresponding author. Tel.: +353 53 9171271.
  E-mail address: owen.fenton@teagasc.ie (O. Fenton).

the most significant anthropogenic sources of NO_3-N contamination in groundwater (Oyarzun et al., 2007). Current agricultural practices (application methods, application rates and storage) while achieving high nutrient efficiency and nutrient management cannot avoid some nutrient losses to surface and groundwater. Contamination of shallow groundwater (<30 m bgl) with NO_3-N has been documented in a large number of studies (C. D. A. McLay et al., 2001; Harter et al., 2002; Bohlke et al., 2007; Babiker et al., 2004). To relate different forms of landuse to different shallow groundwater NO_3-N concentrations spatially, a variety of statistical techniques, such as multivariate cluster analysis (Hussain et al., 2008; Ismail and Ramadan, 1995; Yidana et al., 2008), Tobit and logistic regression using mean nutrient data (Gardner and Vogel, 2005; Kaown et al., 2007), weights of evidence modelling techniques (Masetti et al., 2008), and ordinary kriging methods (Hu et al., 2005), have been used. Other tools, such as regression models based on conceptual models, link shallow groundwater NO_3-N concentration with inventories such as landuse and cattle density (Boumans et al., 2008). Other techniques are employed when both spatial and temporal relationships are considered such as the vulnerability of an aquifer to nitrate pollution through the use of DRASTIC and GLEAMS models (Almasri, 2008; Leone et al., in press). Spatial and temporal correlations of surface and groundwater were described using t-test analysis to show that surface and groundwater management should be integrated (Kannel et al., 2008). Agri-environmental indicators (AEIs) provide information on environmental as well as agronomic performance, which allows them to serve as analytical instruments in research and provide thresholds for legislation purposes Langeveld et al. (2007) investigated AEIs used in various studies: nitrogen use efficiency, nitrogen surplus, groundwater nitrate concentration and residual nitrogen soil concentration, to explain nitrogen management. Results indicated an integrated approach at an appropriate scale should be tested, not forgetting that indicators are simplifications if complex and variable processes.

The land surface around a well which contributes to the water quality at that well may be calculated from: aquifer discharge ($m^3\,day^{-1}$), aquifer thickness (m) and effective Darcian velocity ($m\,day^{-1}$). This circular buffer zone contributes direct recharge to a specific monitoring point, such as a borehole or piezometer (Kolpin, 1997). The circular shape is assumed to be homogenous according to its physical properties. If groundwater flow direction is known, any pollution sources down-gradient of the monitoring point may be discounted. The size of the buffer zone is an important factor and many studies have used different buffer zone radii: (Eckhardt and Stackelberg, 1995) – 800 m; (Kolpin, 1997) – 200 to 2000 m; (Barringer et al., 1990) – 250 m to 1000 m, (McLay et al., 2001) – 500 m and (Kaown et al., 2007) – 73 to 223 m. A mean diameter is often taken where a large range occurs. In an area with a common landuse nutrient management within this area will be an important factor as well as identifying potential point sources in this zone.

Both qualitative and quantitative methods need to be applied to investigate contaminant concentration patterns and to calculate contaminant mass flux. Contaminant flux can prove that natural attenuation occurs on a site but does not differentiate between dilution and denitrification. Contaminant mass flux across a transect of wells, known as a control plane, has been used to quantify the contaminant load leaving a system (Basu et al., 2006; Bockelmann et al., 2001, 2003; Brusseau et al., 2007; Campbell et al., 2006; Duncan et al., 2007; Hatfield et al., 2004; Kubert and Finkel, 2006). This method allows a quantifiable load of NO_3-N leaving a system to be calculated, rather than focusing on a point where shallow groundwater exceeds target or legislative concentration limits such as 11.3 mg NO_3-N L^{-1}.

Traditional source treatment assessment has focused on the pollution source zone, partial mass removal and the calculation of the source strength (contaminant mass discharge and mass flux). Contaminant plume properties are a combination of source strength, assimilative capacity (differential mass discharge with distance along a plume) and time. This procedure is based on the assumption that source treatment results in a contaminant mass reduction in the source zone. It gives an incomplete view of potential impacts and there is uncertainty regarding the plume response to partial mass removal (source treatment). Risk reduction is, therefore, uncertain and the associated costs are difficult to ascertain (Jarsjö et al., 2005). The source strength is calculated from groundwater samples, taken at specified time intervals, and the water flow velocity calculated for each well. These data are then inputted into predictive models and the down-gradient concentration in a sentinel well is predicted. The sentinel well is positioned along a compliance plane down-gradient of the control plane and up-gradient of a potential receptor. For the calculation of contaminant mass flux, a number of screened wells along a control plane, which transect the entire contamination plume perpendicular to groundwater flow direction downstream of the pollutant source, are used, as opposed to the standard central line cross section parallel to groundwater flow direction of the plume (Bockelmann et al., 2003). Longitudinal cross sections may over- or underestimate the contaminant mass flux value and this method requires a larger number of piezometers. The contaminant mass flux is then measured directly from the contaminant flow and concentration in the monitoring piezometers. The source strength is interpolated and then inputted into a model for the prediction of down-gradient contaminant concentrations. Natural attenuation rates (dilution and denitrification) may be achieved by the use of two control planes: a control plane to calculate contaminant mass flux (influent) and a compliance plane down-gradient (Kao and Prosser, 2001). Flux-averaged concentrations along the compliance plane must adhere to specified water quality targets.

The aim of this study was to investigate the factors contributing to the occurrence of elevated NO_3-N concentration in shallow groundwater (<10 m) on a section of a beef farm in SE Ireland. A statistical framework, combining mean geochemical and physical data (saturated hydraulic conductivity (K_{sat}) measurements, ground elevation (m Above Ordnance Datum), elevation of groundwater sampling (screen opening interval) (m AOD) and distance from point pollution source (m)) from a grid of 17 piezometers over a 2 year period, was used to identify factors affecting the occurrence of NO_3-N concentration on site.

The contaminant mass flux entering and leaving the site is also assessed through rows of piezometers called control planes to assess the amount of natural attenuation due to dilution and denitrification combined on site. To differentiate between dilution and denitrification occurrence on site chloride (Cl^-) was also inputted into the model and NO_3/Cl^- ratios investigated. Other parameters were sampled on a random date to confirm areas indicative of denitrification.

1.1. Introduction to the study site

A 4.2 ha gently sloping (2%) study site, comprising six study plots, was located on a beef farm at the Teagasc, Johnstown Castle Environmental Research Centre, Co. Wexford, Ireland (Fig. 1).

The field site is bound to the north by an elevated 3.2 ha grassland sandhill area (71–75 m above ordnance datum (AOD), slope 5%), to the northwest by a 2.8 ha grassland site (71–72 m AOD, slope 2%, and on all other sides by agro-forestry. The dirty water point source was located in this sandhill area.
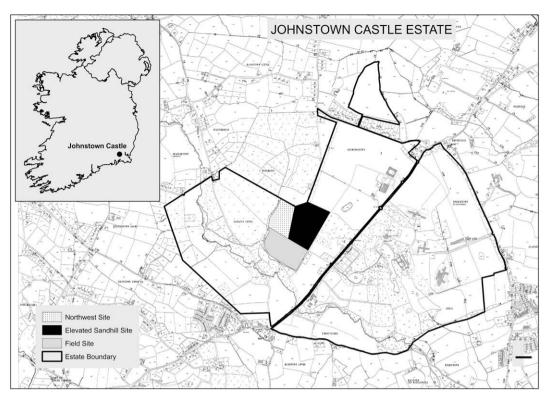
Fig. 1. Field site and northwest and elevated sandhill locations.

Possible receptors on site are a narrow contour stream and the larger Kildavin River boarding the site (Fig. 2). The sandhill and northwest areas are up-gradient and hydrologically connected through shallow flow lines to the 4.2 ha study site approximately 200 m away. Groundwater head contours show groundwater flow direction is towards the six isolated plots (Fig. 2).

Two shallow, unlined trapezoidal drains, excavated to a depth of 1 m, with bases ranging from 71.08 m AOD to 70.2 m AOD and 71.10 m AOD to 70.30 m AOD, respectively, were constructed along the northern edge of the plots. This prevents runoff from entering the plots from the elevated up-gradient area. Runoff from the point source flowed directly into these drains. The plots were also
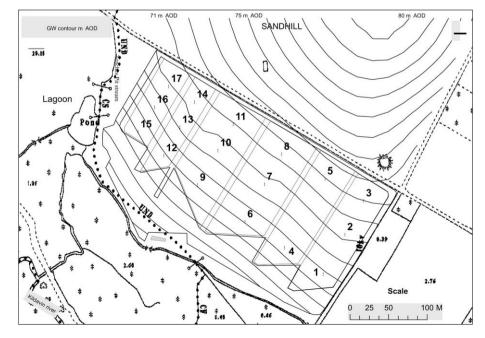

Fig. 2. Field site and elevated sandhill. Groundwater flow map. Sandhill groundwater head contours are based on watertable data from 3 wells drilled in this area. Wells 1, 4, 6, 9, 12 and 15 form the compliance control plane. Wells 3, 5, 8, 11, 14, and 17 form the first control plane. Wells 2, 7, 10, 13 1and 16 form the intermediate control plane.

isolated laterally to 1 m bgl to prevent cross flows from one plot to the other.

Heterogeneous glacial deposits on the farm vary in thickness from 1 to 20 m. On site the glacial deposits are <10 m, underlain by Pre-Cambrian greywacke, schist and massive schistose quartzites, which have been subjected to low grade metamorphism. Outcrop appears just south of the plots and confirms with the shallow nature of the glacial deposits.

This results in a differential K_{sat} at depth. The topography is morainic and, in the area of the point source pollution where the elevation is greater than 71 m AOD, consists of both sand and fine loamy till, and has different topographical form and drift composition. Some of this sand may have been solifucted downslope, resulting in stratification between sand and underlying fine till. The sandhill is well- to excessively drained and consists of deep loamy sands (Fig. 2). A sandpit of industrial grade sand is in operation in the area.

Topsoil samples (0–0.4 m) contained $22 \pm 3.7\%$ coarse sand, $26 \pm 3.6\%$ fine sand, $34 \pm 5.1\%$ silt and $18 \pm 2\%$ clay and subsoil samples (0.4–1.0 m) contained $18 \pm 5.3\%$, $22 \pm 4.2\%$, $34 \pm 4.5\%$ and $25 \pm 4\%$, respectively (Diamond, 1988). Clay content increases with depth on site as sand decreases. Silt content remains the same. Textural changes are not due to pedolocical processes but to small scale sorting of glacial till. It is this transition between sand and clay that governs K_{sat} heterogeneity at depth. Subsoils with a high percentage of fines (clay and silt) are classed as having low permeability, poorly sorted subsoils are assigned as having moderate permeability and well sorted coarse grained subsoils (glaciofluvial sand and gravel) have high permeability (Swartz et al., 1999).

In 2005, the first groundwater samples were taken. (The study site was instrumented with piezometers in 2003.) Initially, 30% of all shallow groundwater samples (<5 m) exceeded NO_3-N drinking water quality targets (11.3 mg NO_3-N l^{-1}). The present model is only applicable to shallow flow lines of the same groundwater age connecting the pollution source to the 1 m screen intervals in all 17 piezometers. (Fenton et al., 2008) investigated the source of pollution and proposed the use of a continuous shallow denitrification trench to intercept contaminated shallow groundwater. A stationary beef dirty water irrigation system, operated on the sandhill for decades until 2004, and was identified as a pollution point source (Fig. 2). This small area has been treated uniformly over a long period of time, before and after implementation of the irrigation system. Currently, the site is cut for silage twice a year and is being used to monitor natural attenuation of the elevated groundwater NO_3-N plume migration, position and concentration on site.

2. Materials and methods

2.1. Nutrient management

A detailed account of organic and inorganic application and silage production on the sandhill, northwest and field site was kept for 2006–2007. Nutrient records confirm uniform treatment in subsequent years. The nitrogen (N) surplus was calculated for each area. These areas are not grazed.

2.2. Monitoring on site

Partially penetrating piezometers ($n = 17$) (25 mm LDPE casing; Van Walt Ltd., Surrey, U.K.) were installed in a grid to shallow groundwater of multilevel depths using rotary drilling (60 mm) (Giddings soil excavation rig, Colorado, USA) to several metres below the groundwater table. The average piezometer drilling

depth was 3.2 m bgl (Table 3), with a 1 m screen at the bottom of each well. The screen was covered with a filter sock, surrounded with washed pea gravel, and sealed with bentonite above the gravel. Two multi level drilling depths were used, from 63 m to 67 m above ordnance datum (AOD), and from 67 m to 70 m AOD, respectively, were drilled.

Drilled holes were back-filled with gravel (3–6 mm diameter) to 0.5 m above the screen, sealed with bentonite (1 m-deep), and then back-filled to the land surface to avoid contamination. All piezometers were surveyed using GPS (X-Y survey only) and the locations of the piezometers were recorded using digital mapping software (ArcGIS™ 9.1, ESRI, Ireland). The site and monitoring network was then digitised using a DGPS antenna, MG-A1 equipment (TOPCON, Ireland) and the site elevations were obtained (Z survey). The depth to the water level in each monitoring well was measured using an electric water-level indicator (Van Walt Ltd, Surrey, U.K.) and groundwater heads were determined using ordnance survey data. Data are described using m AOD to allow comparisons of plume position, thus eliminating topographical differences.

Surface water features, such as streams, drains and lagoons, were also levelled on the same date. The maps were used to construct groundwater maps and elucidate groundwater flow direction. A topographic base map with a field boundary overlay was generated using ArcGIS™ and merged with well location and groundwater head input files. 2-dimensional groundwater data models were generated using GW-Contour 1.0 software (Waterloo Hydrogeologic, Canada).

Watertable levels were measured weekly using an electronic dipper (Van Walt Ltd, Surrey, U.K.) and groundwater was sampled in duplicate using a Waterra hand-held pump (Van Walt Ltd, Surrey, U.K.) Nutrient concentrations were analysed (in duplicate) monthly with a Thermo Konelab 20 (Technical Lab Services, Ontario, Canada) for nitrite-N (NO_2-N), total oxidised N (TON-N), ammonium-N (NH_4-N) and chloride (Cl^-).

2.3. Water balance

A water balance of the site was used to calculate the travel time from surface level to the watertable in the six isolated plots. Daily weather data, recorded at the Johnstown Castle Weather Station, were used to calculate daily soil moisture deficit (SMD) using a Hybrid model for Irish grasslands. Potential evapotranspiration, ET_0 (mm day^{-1}), was calculated using the FAO Penman–Montieth equation (Allen et al., 1998):

$$ET_0 = \frac{0.408\Delta(R_n - G) + \gamma\frac{900}{T+273}u_2(e_s - e_a)}{\Delta + \gamma(1 + 0.34u_2)} \tag{1}$$

where R_n is the net radiation at the crop surface (m^{-2} day^{-1}), T is the air temperature at a 2 m height (°C), u_2 is the wind speed at a 2 m height (m s^{-1}), e_s and e_a are the saturation and the actual vapour pressure curves (kPa °C^{-1}), and γ is the psychrometric constant (kPa °C^{-1}). ET_0 was then converted to actual evapotranspiration (Ae) using an Aslyng scale recalibrated for Irish conditions (Schulte et al., 2005). Effective rainfall was calculated by subtracting daily actual evapotranspiration from daily rainfall (assuming no overland flow losses due to the high infiltration capacity of the soil on this site). Higher K_{sat} zones were found in the topsoil, even in the poorly drained plot. SMD on day one (January 1st, 2006 and 2007) was set to zero and effective drainage was estimated for each subsequent day. Modelling the effective drainage enables the infiltration depth of water to be calculated at specific hydraulic loads where the soil effective porosity is known. This infiltration depth may be compared to watertable data to investigate if recharge to groundwater in that particular year affects water quality.

2.4. Hydraulic conductivity determination

K_{sat} for the open screen area of each piezometer was estimated in slug tests using an electronic diver (Eijkelkamp, the Netherlands) set to record heads at 1-sec time intervals in each piezometer. The diver measures the initial head of water in the piezometer before, during and after the test until full recovery occurs in the piezometer. A slug of 1 L of water was placed instantaneously into the piezometer. The start time (t_0) for the test was noted. Data was downloaded and analysed after (Bouwer and Rice, 1976) method as outlined in (ILRI, 1990) for unconfined aquifers in steady-state flow conditions:

$$K_{sat} = \frac{r_c^2 \, \ln\left(\dfrac{R_e}{r_w}\right)}{2d} \frac{1}{t} \ln \frac{h_0}{h_t} \tag{2}$$

where r_c is radius of the unscreened part of the well where the head is rising, r_w is the horizontal distance from the well centre to the undisturbed aquifer, R_e is the radial distance over which the difference in head, h_o, is dissipated in the flow system of the aquifer, d is the length of the well screen, h_o is the head in the well before the start of the test and h_t is the head in the well at time $t > t_0$.

As the wells on site are partially penetrating, the following equation was used:

$$\ln \frac{R_e}{r_w} = \left[\frac{1.1}{\ln\left(\dfrac{b}{r_w}\right)} + \frac{A + B \ln\left[\dfrac{(D-b)}{r_w}\right]^{-1}}{\dfrac{d}{r_w}} \right] \tag{3}$$

where b is the distance from the watertable height to the bottom of the well, D is the distance from the watertable to the impermeable zone, and A and B are dimensionless parameters, which are function of d/r_w. If $D >> b$, the effective upper limit of $\ln[(D-b)/r_w]$ may be set to 6. A spatial K_{sat} map was developed in ArcGIS™ and merged with well location and groundwater head input files. b is measured by an electronic dipper before commencement of the slug test.

2.4.1. Discharge and Darcian velocity

The quantity of water discharging from each plot (a known width of aquifer), Q ($m^3 \, day^{-1}$), was determined using (Darcy, 1856):

$$Q = -K_{sat} \, A\frac{dh}{dx} \tag{4}$$

where $A = bw$, where b is the aquifer thickness (m), w, the width (m), and dh/dx is the hydraulic gradient. w is taken as the combined diameter of the plots.

The average effective Darcian linear velocity, v ($m \, day^{-1}$), was calculated from:

$$v = -K_{sat} \frac{1}{n} \frac{dh}{dx} \tag{5}$$

where v is equal to Q/A, and n is effective porosity calculated in a previous study by (Fenton et al., 2008).

The transmissivity, T ($m^2 \, day^{-1}$), was calculated using the aquifer thickness, b:

$$T = K_{sat} b \tag{6}$$

2.4.2. Buffer zone diameter and contaminant mass flux

A land use circular buffer zone around each piezometer was previously used to correlate a landuse area that contributes to groundwater quality (Kaown et al., 2007) where the diameter D (m) of the buffer zone in the direction of groundwater flow was approximated by:

$$D = \frac{Q}{bv} \tag{7}$$

where Q is calculated using Equation (4), b is the aquifer thickness as used in Equation (6) and v is calculated using Equation (5). The central piezometer in each plot was taken as the centre of the buffer area. In areas where groundwater flow direction is known the buffer zone method over estimates the groundwater contribution down hydraulic gradient, while underestimating the area of contribution up hydraulic gradient, which should extend to a groundwater divide. When groundwater flow direction is known the buffer zone becomes a true zone of contribution (ZOC). This is then defined as the area surrounding the piezometer that encompasses all areas or features that supply groundwater recharge to the piezometer up hydraulic gradient to the groundwater divide. In this case the groundwater divide is represented by the brow of the sandhill. Over a period of time, determined by effective Darcian velocity, groundwater within the ZOC will flow past the piezometer monitoring point and thus will affect the hydrochemistry at that point. In this study land use management within the entire ZOC, was assessed.

To evaluate the contaminant mass flux ($g \, m^3 \, day^{-1}$) of a dissolved contaminant, the mass flux was measured across a control plane (row of piezometers). The total contaminant mass flux across a control plane was determined by summing the mass flux of the individual cells along this plane. Each cell was assigned a unique depth of saturated zone, mean NO_3-N concentration, and groundwater-specific discharge (calculated using mean K_{sat} values at each piezometer and mean hydraulic gradient in each plot). The total mass flux across the plane was determined by summing the mass flux of the individual plots according to (API, 2003):

$$w = \sum_{i=1}^{i=n} C_i q_i A_i \tag{8}$$

where w is total mass flux across a control plane ($g \, m^3 \, day^{-1}$), C_i concentration of constituent in ith plot ($g \, L^{-1}$), q_i is specific discharge in ith plot ($m \, day^{-1}$) and A_i is area of ith plot (m^2). Within the plots, three control planes were assigned using the top (3, 5, 8, 11, 14, 17), middle (2, 7, 10, 13) and bottom (1, 4, 6, 9, 12 and 15 form the compliance control plane) piezometers (Fig. 2). The contaminant mass flux passing through each control plane was calculated and the natural attenuation process assessed.

The overall efficiency of NO_3-N attenuation between control planes has been used in riparian studies (Orleans et al., 1994; Dhondt et al., 2006) and may be calculated by the following equation:

$$Efficiency = \frac{N_{IN} - N_{OUT}}{N_{IN}} * 100\% \tag{9}$$

where N_{IN} is the up-gradient NO_3-N contaminant mass flux and N_{OUT} is the down-gradient contaminant mass flux.

2.5. TOBIT regression

The effects on groundwater NO_3-N concentration of K_{sat} ($m \, day^{-1}$), elevation, screen opening elevation and distance from pollution source were assessed using a Tobit regression model (Tobin, 1958). The NO_3-N concentration was left censored using a background concentration threshold of 2.6 $mg \, L^{-1}$. Model selection was performed using a forward selection stepwise procedure. Due to the grid layout of the piezometers, residuals could not be assumed to be independent and their spatial dependence was modelled using an anisotropic power covariance structure. The anisotropic power correlation model depends on two parameters: one that represents the correlation between piezometers in the direction of rows and the other that represents the correlation in

the direction of columns. Models were fitted using the MIXED procedure (SAS, 2003). To separate the effect of groundwater NO_3-N denitrification from dilution, groundwater NO_3-N retention is studied by evaluating concurrently groundwater NO_3-N and Cl^- concentration (Altman and Parizek, 1995). To investigate the effect of dilution on the study area Cl^- was also inputted into the model. Cl^- is considered a conservative tracer.

2.6. Denitrification

Denitrification is considered the most important reaction for NO_3^- remediation in aquifers. The process of denitrification occurs in O_2 depleted layers with available electron donors and in agricultural environments with N nutrient losses considerable NO_3^- reduction is possible. To investigate further if denitrification is a viable pathway for NO_3^- reduction some additional water quality measurements were taken on a random date. Physio-chemical parameters-pH, redox potential (Eh (mV)), conductivity (cond ($\mu S\,cm^{-1}$)), temperature (temp (°C)) and rugged dissolved oxygen (RDO ($\mu g\,L^{-1}$)) were measured in the field using a multi parameter Troll 9500 probe (In-situ, Colorado, U.S.A) with a flow through cell.

To elucidate the locations of potential denitrification during groundwater sampling based on dissolved N_2 and the N_2/Ar ratio, three water samples were taken from each piezometer mid way within the screened interval using a 50 ml syringe and gas impermeable tubing. Samples were transferred from the syringe to a 12 ml Exetainer® (Labco Ltd, UK) and sealed to avoid any air entrapment with a butyl rubber septum. Samples were then placed under water in an ice box, transported to laboratory and kept in a cold room at 4 °C prior to analysis. Dissolved N_2, O_2 and Ar were analysed using a Membrane Inlet Mass Spectrometry (MIMS) at the temperature measured (11 °C) during groundwater sampling (Kana et al., 1994). For N_2O concentration, three additional samples were taken in glass bottles for degassing. Eighty ml collected water was injected into a pre-evacuated 160 ml serum bottle followed by 80 ml pure helium. The bottles were shaken for 5 min and then 15 ml equilibrated gas in the headspace was collected using an airtight syringe and transferred into a 12 ml Exetainer for the analysis of dissolved N_2O using a gas chromatography (GC; Varian 3800, USA) equipped with electron capture detector. The concentration of dissolved N_2O was calculated by using the Henry's law constant, the concentration of the gas in the head space, the bottle volume, and the temperature of the sample but the lowest 14 °C was taken due to limitation in gas solubility coefficient to calculate Henry's law constant (Hudson, 2004).

3. Results

3.1. Nutrient management

In 2006 as in previous years after the point source was removed, the sandhill area, the northwest area and the isolated plots received the same N application (Table 1). These areas were cut for first cut silage at the end of May and for second cut silage in July but they were not grazed by cattle for the duration of this study. Half of the fertiliser N was applied as urea in late-February and April and the remaining N was applied in June and August as calcium ammonium nitrate (CAN). Loss of N to the environment from urea would tend to be atmospheric ammonia (NH_3) losses as urea tends to be immobile and is retained in the soil by cation exchange capacity (CEC). Whereas N applied as CAN is already partially nitrified and would be susceptible to leaching and denitrification.

At a crop uptake rate of $2\,kg\,N\,ha^{-1}\,day^{-1}$ from March–May, a surplus of approximately $75\,kg\,N\,ha^{-1}$ remained after first cut silage. The grass needed approximately $80\,kg\,N\,ha^{-1}$ before second

Table 1
Nutrient management of the sandhill, northwest and field site for 2006 and 2007.

Year	Location	Area (ha)	Month	N fertiliser application rate (kg N ha^{-1})	Nitrogen fertiliser type
2006					
	Sandhill	3.2	Feb	28.5	Urea[a]
			April	124.1	Urea
			June	102.1	CAN[b]
			Aug	51.1	CAN
	Northwest	2.8	Feb	28.5	Urea
			April	124.1	Urea
			June	102.1	CAN
			Aug	51.1	CAN
	Plots	4.2	Feb	28.5	Urea
			April	124.1	Urea
			June	102.1	CAN
			Aug	83.7	CAN
2007					
	Sandhill	3.2	March	56.9	Urea
			April	71.2	Urea
			June	102.1	CAN
			Aug	51.1	CAN
	Northwest	2.8	March	56.9	Urea
			April	124.1	Urea
			June	102.1	CAN
			Aug	51.1	CAN
	Plots	4.2	March	28.5	Urea
			April	124.1	Urea
			June	102.1	CAN
			Aug	83.7	CAN

[a] Urea is 46% nitrogen.
[b] Calcium Ammonium Nitrate (CAN) is 27% nitrogen.

cut silage at the end of July. Therefore, no N leaching losses would be expected from this surplus. In August 2006, the six isolated plots received a higher application of CAN ($83.7\,kg\,N\,ha^{-1}$) for the third cut silage in early October. The grass requirement for third cut silage matched the fertiliser application rate (approximately $90\,kg\,N\,ha^{-1}$).

In June 2007, in addition to fertiliser application (Table 1), the sandhill and northwest area received $118\,kg\,N\,ha^{-1}$ as cattle slurry. The sandhill area was N-deficient by approximately $24\,kg\,N\,ha^{-1}$ for first cut silage in May. With addition of CAN and slurry in June, there was an N-surplus of approximately $70\,kg\,N\,ha^{-1}$ after second cut silage. In July and August 2007, there was a large increase in effective drainage. With the time lag between second cut silage and the final application of CAN in the middle of August, there was just enough N available for grass recovery. The same was true for the northwest site but there was a surplus after first cut silage in May.

3.2. Water balance

A water balance for the site showed total precipitation of 992.6 mm and 889.1 mm for 2006 and 2007, respectively. For the two years, the Hybrid model calculated 483 mm and 335 mm drainage through the root zone in a process known as effective drainage. It was assumed that all of this direct recharge reached the watertable as the rainfall intensity is generally lower than the soil infiltration capacity. Model output showed effective drainage occurred on 87 and 74 days, giving an average recharge rate of 5.5 and $4.5\,mm\,day^{-1}$, respectively. Cumulative drainage for both years is presented in Fig. 3. The mean soil total porosity was $32.2 \pm 4.9\%$. The average pore velocity was estimated to be 17.3 and 14.1 mm day^{-1}, giving an approximate mean travel depth of 1.5 and 1.04 m in
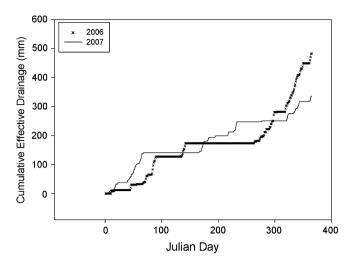
Fig. 3. Calculated cumulative effective drainage (mm) from 2006 to 2007.

a moderately drained soil for 2006 and 2007. The mean watertable depth for 2006–2008 on site was 2.2 m bgl. This is the unsaturated zone vertical travel time (approx 2 years) achievable due to effective drainage, representative of drainage during the winter period. Lateral migration of the nutrients is with groundwater flow direction under the experimental plots.

Accumulative effective drainage shows differential recharge each year and seasonal differences in recharge led to differential NO_3-N dilutions over time. Both years had wet winters but 2006 had a dry summer period (Fig. 3). Slurry was only spread in times of dry weather. This contributed to higher mean site NO_3-N concentrations for sampling events in early 2006. The dry summer of 2006 halted significant recharge and NO_3-N concentrations reached steady state. As effective drainage increases, overall mean NO_3 concentration on site increases.

Each piezometer followed the same pattern for mean NO_3-N concentration, with some piezometers falling below the 11.3 mg L^{-1} threshold for drinking water quality within 1 year. There was no increase in the shallow groundwater NO_3-N concentration, after the slurry application in June 2007 due to a combination of slow groundwater transport (K_{sat} ranges from 0.001 to 0.016 m day^{-1} with subsequent travel distance of 2.9 and 4.5 m yr^{-1}) (Table 2) and gaseous losses of NH_3.

3.3. Buffer zone and contaminant mass flux

Buffer zone diameter for plots 1–6, using Equation (7), was 193, 178, 195, 195, 148 and 120 m respectively.

A mean area of 2.4 ha for the ZOC was calculated. The buffer zones can extend beyond the isolated study site to the groundwater divide in the sandhill area. Therefore, land management and recharge in the entire ZOC area can contribute to shallow groundwater NO_3-N contamination within the study site. The historical stationary dirty water point source pollution occurred within this ZOC.

The contaminant mass fluxes calculated for three control planes are presented in Table 2. Influent contaminant mass flux through the upper control plane cells ranged from 0.0008 to 0.0016 g N m^3 day^{-1} and the contaminant mass fluxes leaving the site at the compliance plane ranged from 0.00001 to 0.0007 g N m^3 day^{-1}. Total contaminant mass flux on a plot basis was as follows: Plot 3 > 1 > 5 > 4 > 6. Total contaminant mass flux decreased from the top plane to the central plane to the compliance plane demonstrating natural attenuation. Using Equation (9), a 42% contaminant mass flux reduction efficiency was calculated from the influent control plane to the central plane. From the central plane to the compliance plane a 64% reduction occurred. Plot 3 contributed the greatest contaminant mass flux. The load transfer from the influent control plane to the central control plane showed a reduction of 33.6%, with a subsequent reduction of 69.5% at the compliance control plane. Plot 4 showed a 96% reduction in contaminant mass flux from the influent control plane and the central control plane. Plot 1 doubled its contaminant mass flux from the influent control plane to the central control plane, but then decreased by 51.2% down-gradient at the compliance control plane. The upper, middle and lower control planes are 18%, 44% and 76% below the compliance control plane threshold (11.3 mg L^{-1} with present flux) respectively.

4. TOBIT regression

Selected piezometer parameters are presented in Table 3. In each step of the procedure, a series of regressions are fitted (Table 4). Each model includes random effects to account for the spatial dependence of model residuals. Type III F-tests for the fixed effects are presented for each model accompanied by Akaike's Information Criterion (AIC). The AIC is a model selection tool that compares the Log Likelihood of models while penalising for the number of

Table 2
Contaminant mass flux calculation for six isolated plots.

Parameters	Plot number					
	1	2	3	4	5	6
Area (ha)	0.78	0.75	1.01	0.94	0.41	0.41
Width of plot (m)	50	50	55	55	30	30
Mean effective velocity v (m day^{-1})	0.011	0.006	0.012	0.013	0.012	0.008
Hydraulic conductivity K (m day^{-1})	0.009	0.0083	0.0117	0.0117	0.0123	0.008
Transmissivity T (m^2 day^{-1})	0.07	0.07	0.09	0.09	0.1	0.06
Mean hydraulic head (Top) (m AOD)	67.13	68.65	70.13	69.92	69.53	69.3
Mean hydraulic head (Bottom) (m AOD)	63.31	66.21	66.8	66.4	66.5	66.28
Mean Travel Distance in 1 year	3.92	2.31	4.44	4.70	4.25	2.76
Q	m^3 day^{-1}					
Top Control Plane Nodes	0.15	0.15	0.15	0.15	0.12	0.09
Middle Control Plane Nodes	0.15	–	0.15	0.20	0.11	0.07
Bottom Control Plane Nodes	0.11	0.01	0.22	0.19	0.04	0.01
Contaminant Mass Flux	g m^3 day^{-1}					
Top Control Plane Nodes	0.0009	0.0017	0.0016	0.0009	0.0015	0.0008
Middle Control Plane Nodes	0.0018	–	0.0011	0.0001	0.0010	0.0004
Bottom Control Plane Nodes	0.00074	0.00001	0.0003	0.0000	0.0004	0.0001

Table 3
Selected piezometer parameters from 2005 to 2008.

Piezometer	Plot	Position	Total depth (m bgl)	Elevation (mAOD)	Mean NO$_3$-N (mg L^{-1})	Stdev±	Mean NO$_2$-N (mg L^{-1})	Stdev±	Mean Cl$^-$ (mg L^{-1})	Stdev±	Mean NH$_4$-N (mg L^{-1})	Stdev±	Mean NO$_3$-N/Cl$^-$ ratio	Stdev±	K_{sat} (m day^{-1})	Mean Watertable Elevation (mAOD)
1	1	Bottom	3.6	67.8	6.9	2.7	0.04	0.1	27.1	6.1	0.24	0.3	0.08	0.25	0.007	63.7
2	1	Middle	4.1	70.2	11.6	4.9	0.05	0.2	24.9	7.4	0.25	0.6	0.09	0.48	0.01	66.9
3	1	Top	4.3	72.1	5.6	3.5	0.07	0.1	18.4	4.8	0.34	0.3	0.25	0.30	0.01	67.9
4	2	Bottom	3.1	67.6	1.4	3.5	0.07	0.0	28.8	8.1	1.67	1.1	0.18	0.10	0.001	66.3
5	2	Top	4.3	72.0	11.8	5.7	0.02	0.0	19.0	5.2	0.21	0.5	0.27	0.62	0.015	68.8
6	3	Bottom	3.5	68.2	12.8	3.4	0.09	0.2	32.5	5.5	0.26	0.4	0.09	0.41	0.015	66.6
7	3	Middle	2.6	70.0	7.3	2.6	0.01	0.0	19.0	10.4	0.06	0.1	0.08	0.43	0.01	68.5
8	3	Top	3.2	71.7	11.0	3.4	0.03	0.1	59.0	9.5	0.22	0.4	0.04	0.53	0.01	69.6
9	4	Bottom	2.7	67.7	0.1	1.3	0.01	0.0	9.9	10.6	0.16	0.1	0.06	0.02	0.012	65.1
10	4	Middle	2.9	69.5	0.3	1.5	0.00	0.0	41.4	6.3	0.10	0.1	0.06	0.01	0.013	67.9
11	4	Top	2.4	71.8	5.7	2.7	0.00	0.0	21.9	7.8	0.06	0.2	0.08	0.24	0.01	70.3
12	5	Bottom	1.5	67.7	8.7	2.3	0.01	0.0	32.5	7.2	0.08	0.1	0.07	0.27	0.006	65.6
13	5	Middle	2.8	69.4	9.4	2.7	0.00	0.0	29.1	4.9	0.07	0.1	0.09	0.32	0.015	68.2
14	5	Top	4.3	72.0	12.8	4.1	0.02	0.1	30.2	2.9	0.24	0.4	0.15	0.47	0.016	71.0
15	6	Bottom	2.9	67.4	3.6	2.7	0.02	0.0	33.9	4.1	0.23	0.4	0.08	0.10	0.002	64.0
16	6	Middle	3.1	68.4	5.0	1.7	0.04	0.1	24.5	6.4	0.14	0.2	0.11	0.19	0.01	67.1
17	6	Top	3.0	71.1	9.3	2.0	0.04	0.1	23.2	12.2	0.12	0.5	0.13	0.41	0.012	70.2

parameters in the model. The model with the lowest AIC is the best fitting model.

When assessed individually, K_{sat} ($p = 0.0004$) had significant impacts on NO$_3$-N concentrations. However, K_{sat} ($p = {<}0.001$) and distance from point source ($p = 0.0014$) are significant when K_{sat} is already in the model. The stepwise procedure selected the K_{sat} and distance from point source as having more explanatory power than when other parameters are inputted into the model. The final model contains only K_{sat} and distance from point source. The final model is presented in Fig. 4.

Estimated model coefficients for final model from the Tobit regression are presented in Table 5. The model describes the relationship between mean groundwater NO$_3$-N concentration and the explanatory variables K_{sat} and distance from pollution source. The percentage variation explained by different factors is presented in Table 6.

Dilution due to recharge occurred for all piezometers within the contamination plume on site (NO$_3$-N/Cl$^-$ ratio), but at the same rate for each piezometer. Therefore, dilution did not account for differences in NO$_3$-N concentration within the contamination plume. Therefore, diffuse pollution due to fertiliser application within the field site may be discounted. A two-layered conceptual model represents a shallow zone of higher $K_{sat} \geq 0.01$ m day^{-1} with higher NO$_3$-N concentrations and a deeper low K_{sat} zone ${<}0.01$ m day^{-1} with lower NO$_3$-N concentrations. In the shallow layer, K_{sat} values ranged from 0.01 to 0.016 m day^{-1} but were not consistent with depth, indicating heterogeneity.

4.1. Dilution and denitrification differentiation

In some locations the Cl$^-$ concentration is representative of natural background levels (NBL). In Ireland groundwater has a median NBL of 18 mg L^{-1}. Some points therefore were not included in the regression process. Plots 1, 2, 4, 5 and 6 have the highest ratio in the top of the plots nearest the source but standard deviation shows some change over time (Table 3).

The model was run a second time to explain Cl$^-$ occurrence using the same parameters as before. Here K_{sat} and ground elevation have the greatest explanatory power but K_{sat} is not significant. As shown previously, NO$_3$-N occurrence in the same piezometers was explained by K_{sat} and distance from the dirty water point pollution source pollution, while both being significant. Due to the fact that K_{sat} influences NO$_3$-N occurrence but not Cl$^-$ occurrence denitrification can be inferred. But distances from the dirty water source and ground elevation are linked due to the nature of the sloped site and therefore dilution is a factor for Cl$^-$ occurrence. In general on site:

- Low NO$_3$ concentration and unaffected Cl- concentration points to denitrification (Fig. 5a)
- Low NO$_3$ concentration and low Cl-chloride concentration points to dilution (Fig. 5b)
- Over lying Fig. 5a and b allows areas of denitrification and dilution to be inferred (Fig. 5c)

The Nitrate/chloride ratio identifies two zones where the present plume position is evident. This ratio is low in plot 4 and in the southern part of the site where the plume has not reached. This infers denitrification in the central part of the site (plot 4) and dilution in other areas.

To further elucidate the effect of groundwater denitrification on NO$_3$-N occurrence on the site, dissolved gases and physio-chemical properties of groundwater collected on a random date were determined and related to the mean groundwater NO$_3$-N concentration during the study. Average groundwater NO$_3$-N was

Table 4
Details of the stepwise procedure used to select the explanatory variables of importance in the relationship between mean groundwater NO_3-N concentration and hydrogeological factors. Model containing K_{sat} and distance from point source is chosen as the final model.

Step 1	Include all variables individually in model		Step 3	Add other variables to model containing K_{sat} and distance from point source (m)	
Effect	F(1,11)	P-value	Effect	F(1,9)	P-value
K_{sat} (m day^{-1})	24.55	0.0004	K_{sat} (m day^{-1})	53.5	<0.0001
Elevation (m AOD)	10.23	0.0085	Distance from point source (m)	9.68	0.0125
Distance from point source (m)	0.6	0.4562	Elevation (m AOD)	0.08	0.7884
Screen depth (m AOD)	1.28	0.2826			
			K_{sat} (m day^{-1})	73.45	<0.0001
Result of step 1	K chosen as most important		Distance from point source (m)	15.79	0.0032
			Screen depth (m AOD)	1.69	0.2253
Step 2	Add other variables to model containing K		Result of step 3	Other variables not significant in a model that contains K_{sat} and distance from point source	
Effect	F(1,10)	P-value			
K_{sat} (m day^{-1})	13.05	0.0048			
Elevation (m AOD)	1.75	0.2156			
K_{sat} (m day^{-1})	78.85	<0.0001			
Distance from point source (m)	19.1	0.0014			
K_{sat} (m day^{-1})	33.75	0.0002			
Screen depth (m AOD)	1.47	0.2526			
Result of Step 2	Distance is significant when K_{sat} is already in the model				

significantly ($P < 0.05$) related to groundwater N_2/Ar ratio, redox potential (Eh), dissolved O_2 and N_2 and was close to being significant with dissolved N_2O concentration ($P = 0.08$) (Table 7). Based on the AIC score N_2/Ar ratio and redox potential (Eh) were the best fitting models of groundwater NO_3-N occurrence. The higher ratio of N_2/Ar directly indicates that denitrification is occurring on the site (Fig. 5d) and that lower redox potentials and dissolved oxygen are related to lower groundwater NO_3-N occurrence (Table 7).

5. Discussion

Documented nutrient management of the study site, while contributing to the elevated NO_3-N concentration in shallow groundwater, could not solely account for NO_3-N distribution on site. Surplus nutrients calculated for 2007 in the sandhill area had not yet reached the shallow groundwater under the plots due to slow travel times. Historic dirty water irrigation occurred on the
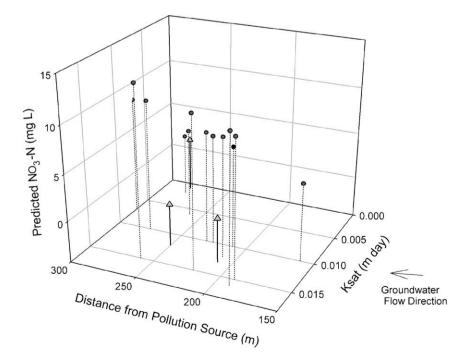

Fig. 4. Predictions of NO_3-N from fitted model.

Table 5
Estimated model coefficients for final NO_3-N model but also for Cl^- from the regression.

Effect	Coefficient	Standard error	Degrees of freedom (DF)	t-value	P-value
NO_3-N					
Intercept	−13.7328	3.6584	0	−3.75	
K	960.98	108.22	10	8.88	<0.001
Distance	0.0506	0.01158	10	4.37	0.0014
Cl^-					
Intercept	212.34	62.22	0	3.41	
K	548.59	390.49	12	1.40	0.1854
Elevation	−2.73	0.9294	12	−2.94	0.0123

sandhill site for decades prior to this study with excessive hydraulic loads leading to elevated infiltration on the sandhill.

Vertical unsaturated zone travel time was not within a single drainage season. Saturated shallow groundwater and contamination plume migration time was from 2.92 to 4.50 m yr^{-1} underneath the plots. The travel time from the sandhill (source) to the plots approximately 200 m away was much quicker due to the sand.

Dilution of the groundwater NO_3-N concentrations by recharge to the shallow watertable occurred in both study years. A two-layered conceptual model of the site emerged, where higher NO_3-N concentrations existed in the shallower, high K_{sat} subsurface.

The model describes the relationship between mean groundwater NO_3-N concentration and the explanatory variables K_{sat} and distance of the piezometers from the point pollution source. To account for bias due to the distance of each piezometer within the grid pattern from the pollution source, the spatial dependence of residuals was modelled using an anisotropic power covariance structure. Higher K_{sat} zones in the subsurface allow faster migration of contaminated groundwater, resulting in shorter retention time. The shorter retention time in the high K_{sat} zone decreases the opportunity for denitrification to occur. Lateral flow in higher K_{sat} layers may result in surface water pollution. The opposite is true of lower K_{sat} zones, where a longer retention time is available for denitrification to occur. This is why low NO_3-N concentrations may be present at the plume centroid. In elevated areas, the watertable mirrors topography and has a greater hydraulic gradient and higher K_{sat} values.

Groundwater NO_3-N occurrence was statistically related to topsoil denitrifying enzyme activity, topsoil inorganic N content, depth to water table and a stronger relationship was observed with vadose zone permeability (McLay et al., 2001). The effect of vadose zone permeability on groundwater NO_3-N distribution was recognised by (Vellidis et al., 1996) who observed low N leaching associated with low subsoil permeability and (Hansen and Djurhuus,

Table 6
Percentage variation explained by different factors.

Fixed	Degrees of freedom	SS	% variation
K_{sat} (m day^{-1})	1	63.72	55.5
Distance from point source (m)	1	15.52	13.3
Screen depth (m AOD)	1	5.48	4.8
Elevation (m AOD)	1	0.62	0.5
Random			
Row	1	7.95	6.9
Column	1	4.26	3.7
Residual	5	17.58	15.3
	Total	114.90	

1996) observed high N leaching with high subsoil permeability. (Richards et al., 2005) observed lower groundwater NO_3-N occurrence in deeper wells with clay soils with no cropland nearby but they could not separate the effect of K_{sat} from landuse or well depth. In Ireland (Ryan and Fanning, 1996) also highlighted the importance of soil type and permeability with lower NO_3-N losses from soil with the percentage fines (silt and clay) >75% estimated mean subsoil travel times of 0.01 m day^{-1} on a site with elevated groundwater NO_3-N concentrations. The unsaturated vadose zone transport of NO_3-N is clearly influenced by the permeability and thus longer residence time in lower permeability subsoil favouring NO_3-N reduction through denitrification. The strong relationship observed in this work also clearly identifies the importance of the saturated subsoil zone in favouring NO_3-N reduction by denitrification in low subsoil permeable zones. Also importance is the exact location of the point pollution source. The strong correlations between mean groundwater NO_3-N and denitrification end products (N_2O and N_2) and physio-chemical properties favouring denitrification (dissolved O_2 and Eh) further supports that denitrification is the dominant process controlling groundwater NO_3-N occurrence and transport on the study site. The relationship between subsoil/aquifer K_{sat} and denitrification requires further investigation.

In Ireland, groundwater protection is based on the mapping of vulnerability zones for the protection of groundwater source (wells and springs) and the groundwater resource. Irish aquifers are deemed to have low attenuation potential due to their fractured and karstified nature and thus they are mainly protected by the overlying glacial tills. Vulnerability zones are ranked in four classes from extreme to low vulnerability based primarily on the thickness and lithology/permeability of the Quaternary subsoil deposits (Daly and Warren, 1988). Vulnerability decreases with increasing thickness and decreasing permeability of subsoil. The definition of groundwater in Ireland often excludes the shallow groundwater in subsoils (with the exception of sand and gravel aquifers) as it is not valued as a potential source of water for human consumption. Although not sufficient for consumption shallow subsoil groundwater is environmentally important as it contributes to through flow and drain flow to surface waters bypassing any potential for abatement when transported through deeper aquifers.

Groundwater protection in Ireland for subsoil permeability is not routinely measured in Irish subsoils, (Fitzsimons and Misstear, 2006) classified Irish till permeability as being highly permeable $K_{sat} = 10$ m day^{-1}, moderately permeable when $K_{sat} = 0.004–0.009$ m day^{-1} and low permeability (clay content >13%) when $K_{sat} = 0.0004–0.0009$ m day^{-1}. Mean plot K_{sat} values on site range from 0.008 from 0.01 m day^{-1}. This suggests further classification may be needed from moderate to highly permeable classes.

Contaminant mass flux calculations show that the load of NO_3-N passing through parallel control planes perpendicular to groundwater flow was uneven across the site. A 96% reduction in contaminant mass flux occurred across the control planes in Plot 3. This leads to groundwater NO_3-N loads of acceptable quality leaving the site. Natural attenuation occurred down-gradient in all plots except Plot 1.

In this study subsoil permeability and distance from point source pollution have been clearly identified as significant factors in determining the occurrence of NO_3-N in groundwater. The subsoil on the study classified as moderate permeability and this study highlights the need to further subdivide this category for risk assessment of NO_3-N occurrence in groundwater and transport to surface waters via through flow or artificial drainage. Furthermore as subsoil K_{sat} is incorporated in the contaminant mass flux
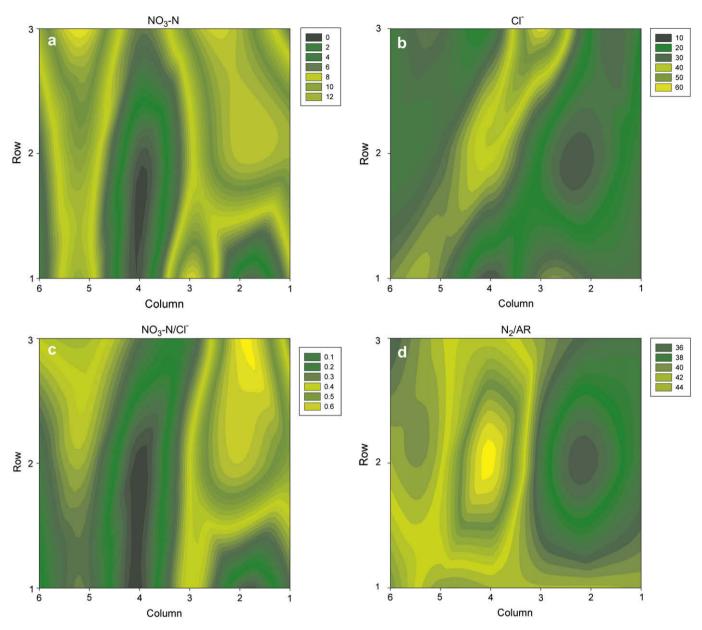
Fig. 5. Spatial distribution across the six plots (x axis) of groundwater a) Mean NO_3-N concentration b) Mean Cl^- concentration c) mean NO_3/Cl^- ratio and d) N_2/Ar ratio on a random date.

calculation, particular hot spot locations may be identified, which contribute significantly more contaminant flux per unit area to potential down-gradient receptors. The identification of hot spots of groundwater contaminants may be used to target areas for locating an environmental remediation technology to reduce contaminant fluxes to sensitive receptors.

6. Conclusion

K_{sat} and distance from point source are important when assessing the spatial distribution of NO_3-N in shallow groundwater. Within subsoils classified as moderately permeable subsoil K_{sat} was significantly related to groundwater NO_3-N occurrence and slight differences in permeability greatly influenced the concentrations on site. Groundwater denitrification is likely to be the dominant process influencing groundwater NO_3-N occurrence and transport at this site. Calculating contaminant mass flux across more than one control plane is a useful tool to monitor natural attenuation. This tool allows the identification of hot spot areas where intervention other than natural attenuation may be needed to protect receptors.

Table 7
Relationships between dissolved groundwater gases, redox potential (Eh) and average NO_3-N. Each parameter is regressed in turn against average NO_3-N. The spatial structure on the variance covariance matrix is as described for the stepwise regression.

Parameter	Estimate	Standard error	T value $_{13\,DF}$	P>t	AIC
N_2/Ar ratio	−1.33	0.544	−2.45	0.029	81
Redox potential (Eh)	0.040	0.013	3.17	0.0073	86.4
N_2O	0.2247	0.1182	1.9	0.0798	87
RDO	0.0012	0.0003	3.58	0.0034	91.4
O_2	0.0011	0.0004	2.48	0.0275	95
N_2	−0.0012	0.001	−2.17	0.0493	95.5

Acknowledgements

References

Allen, R.A., Pereira, L.S., Raes, D., Smith, M., 1998. Crop Evapotranspiration. Guidelines for Computing Crop Water Requirements. FAO irrigation and drainage paper 56. FAO, Rome, Italy, 300 pp.

Almasri, M.N., 2008. Assessment of intrinsic vulnerability to contamination for Gaza coastal aquifer, Palestine. Journal of Environmental Management 88, 577–593.

Altman, S.J., Parizek, R.R., 1995. Dilution of non-point source nitrate in groundwater. Journal of Environmental Quality 24, 707–718.

API, 2003. Groundwater Remediation Strategies Tool. 80 pp.

Babiker, I.S., Mohamed, M.A.A., Terao, H., Kato, K., Ohta, K., 2004. Assessment of groundwater contamination by nitrate leaching from intensive vegetable cultivation using geographical information system. Environment International 29, 1009–1017.

Barringer, T., Dunn, D., Battaglin, W., Vowinkel, E., 1990. Problems and methods involved in relating land use to groundwater quality. Water Resources Bulletin 26, 1–9.

Basu, N.B., Rao, P.S., Poyer, I.C., Annable, M.D., Hatfield, K., 2006. Flux-based assessment at a manufacturing site contaminated with trichloroethylene. Journal of Contaminant Hydrology 86, 105–127.

Bockelmann, A., Ptak, T., Teutsch, G., 2001. An analytical quantification of mass fluxes and natural attenuation rate constants at a former gasworks site. Journal of Contaminant Hydrology 53, 429–453.

Bockelmann, A., Zamfirescu, D., Ptak, T., Grathwohl, P., Teutsch, G., 2003. Quantification of mass fluxes and natural attenuation rates at an industrial site with a limited monitoring network: a case study. Journal of Contaminant Hydrology 60, 97–121.

Bohlke, J.K., O'Connell, M.E., Prestegaard, K.L., 2007. Ground water stratification and delivery of nitrate to an incised stream under varying flow conditions. Journal of Environmental Quality 36, 664–680.

Boland, D., Buijze, S., 2002. Farming on good groundwater: a methodology for cost effective groundwater protection. In: Steenvoorden, J., Claessen, F., Willems, J. (Eds.), Agricultural Effects on Ground and Surface Waters: Research at the Edge of Science and Society.

Boumans, L., Fraters, D., van Drecht, G., 2008. Mapping nitrate leaching to upper groundwater in the sandy regions of The Netherlands, using conceptual knowledge. Environmental Monitoring and Assessment 137, 243–249.

Bouwer, H., Rice, C., 1976. A slug test for determining hydraulic conductivity of unconfined aquifers with completely or partially penetrating wells. Water Resources Research 12, 423–428.

Brusseau, M.L., Nelson, N.T., Zhang, Z., Blue, J.E., Rohrer, J., Allen, T., 2007. Source-zone characterization of a chlorinated-solvent contaminated Superfund site in Tucson, AZ. Journal of Contaminant Hydrology 90, 21–40.

Campbell, T.J., Hatfield, K., Klammler, H., Annable, M.D., Rao, P.S., 2006. Magnitude and directional measures of water and Cr (VI) fluxes by passive flux meter. Environment Science Technology 40, 6392–6397.

Daly, D., Warren, W.P., 1988. Mapping Groundwater Vulnerability: the Irish Perspective. Geological Society London, London, 179–190 pp.

Darcy, H., 1856. Les fontaines publiques de la ville Dijon. Paris.

Dhondt, K., Boeckx, P., Verhoest, N.E.C., Hofman, G., Van Cleemput, O., 2006. Assessment of temporal and spatial variation of nitrate removal in riparian zones. Environmental Monitoring and Assessment 116, 197–215.

Diamond, J., 1988. Soils and Land Use-Johnstown Castle Estate. Teagasc. 16.

Duncan, P.B., Greenberg, M.S., Leja, S., Williams, J., Black, C., Henry, R.G., Wilhelm, L., 2007. Case study of contaminated groundwater discharge: how in situ tools link an evolving conceptual site model with management decisions. Integrated Environmental Assessment and Management 3, 279–289.

Eckhardt, D.A.V., Stackelberg, P.E., 1995. Relation of groundwater quality to land use on Long Island, New York. Groundwater 33, 1019–1033.

Fenton, O., Healy, M.G., Richards, K., 2008. Methodology for the location of a subsurface permeable reactive barrier for the remediation of point source pollution on an Irish Farm. Tearmann 6, 29–44.

Fitzsimons, V.B., Misstear, D.R., 2006. Estimating groundwater recharge through tills: a sensitivity analysis of soil moisture budgets and till properties in Ireland. Hydrogeology Journal 14, 548–561.

Gardner, K.K., Vogel, R.M., 2005. Predicting ground water nitrate concentration from land use. Ground Water 43, 343–352.

Hansen, E.M., Djurhuus, J., 1996. Nitrate leaching as affected by long term N fertilization on a coarse sand. Soil Use and Management 12, 199–204.

Harter, T., Davis, H., Mathews, M.C., Meyer, R.D., 2002. Shallow groundwater quality on dairy farms with irrigated forage crops. Journal of Contaminant Hydrology 55, 287–315.

Hatfield, K., Annable, M., Cho, J., Rao, P.S., Klammler, H., 2004. A direct passive method for measuring water and contaminant fluxes in porous media. Journal of Contaminant Hydrology 75, 155–181.

Hu, K., Huang, Y., Li, H., Li, B., Chen, D., White, R.E., 2005. Spatial variability of shallow groundwater level, electrical conductivity and nitrate concentration, and risk assessment of nitrate contamination in North China Plain. Environmental International 31, 896–903.

Hudson, F., 2004. Sample preparation and calculation for dissolved gas analysis in water samples using a GC headspace equilibration technique. RKSOP-175, Revision No. 2, 14p. EPA, USA.

Hussain, M., Ahmed, S.M., Abderrahman, W., 2008. Cluster analysis and quality assessment of logged water at an irrigation project, eastern Saudi Arabia. Journal Environmental Management 86, 297–307.

ILRI, 1990. Analysis and Evaluation of Pumping Test Data. ILRI, Wageningen, 345 pp.

Ismail, S.S., Ramadan, A., 1995. Characterisation of Nile and drinking water quality by chemical and cluster analysis. Science of the Total Environment 173–174, 69–81.

Jarsjö, J., Bayer-Raich, M., Ptak, T., 2005. Monitoring groundwater contamination and delineating source zones at industrial sites: uncertainty analyses using integral pumping tests. Journal of Contaminant Hydrology 79, 107–134.

Kana, T.M., Darkenjelo, C., Hunt, M.D., Oldham, J.B., Bennett, G.E., Cornwell, J.C., 1994. Membrane inlet mass spectrometer for rapid high-precision determination of N2, O2, and Ar in environmental water samples. Analytical Chemistry 66, 4166–4170.

Kannel, P.R., Lee, S., Lee, Y.-S., 2008. Assessment of spatial temporal patterns of surface and groundwater qualities and factors influencing management strategy of groundwater system in an urban river corridor of Nepal. Journal of Environmental Management 86, 595–604.

Kao, C.M., Prosser, J., 2001. Evaluation of natural attenuation rate at a gasoline spill site. Journal of Hazardous Materials 82, 275–289.

Kaown, D., Hyun, Y., Bae, G.O., Lee, K.K., 2007. Factors affecting the spatial pattern of nitrate contamination in shallow groundwater. Journal of Environmental Quality 36, 1479–1487.

Kolpin, D.W., 1997. Agricultural chemicals in groundwater of the Midwestern United States: relations to land use. Journal of Environmental Quality 26, 1025–1037.

Kubert, M., Finkel, M., 2006. Contaminant mass discharge estimation in groundwater based on multi-level point measurements: a numerical evaluation of expected errors. Journal of Contaminant Hydrology 84, 55–80.

Langeveld, J.W.A., Verhagen, A., Neeteson, J.J., van Kuelen, H., Conijn, J.G., Schils, R.L.M., Oenema, J., 2007. Evaluating farm performance using agri-environmental indicators: recent experiences for nitrogen management in the Netherlands. Journal of Environmental Management 82, 363–376.

Lee, M., 1999. Surface Hydrology and Land Use as Secondary Indicators of Groundwater Vulnerability. Trinity College Dublin, Dublin.

Leone, A., Ripa, M.N., Uricchio, V., Deák, J., Vargay, Z. Vulnerability and risk evaluation of agricultural nitrogen pollution for Hungary's main aquifer using DRASTIC and GLEAMS models. Journal of Environmental Management in press, corrected proof.

Masetti, M., Poli, S., Sterlacchini, S., Beretta, G.P., Facchi, A., 2008. Spatial and statistical assessment of factors influencing nitrate contamination in groundwater. Journal of Environmental Management 86, 272–281.

McLay, C.D., Dragten, R., Sparling, G., Selvarajah, N., 2001. Predicting groundwater nitrate concentrations in a region of mixed agricultural land use: a comparison of three approaches. Environmental Pollution 115, 191–204.

Orleans, A.B.M., Mugge, F.L.T., Van der Meij, T., Vos, P., Ter Keurs, W.J., 1994. Minder nutrinten in het oppervlaktewater door bufferstroken: ein literatuuranalyse (in Dutch). Rijks-Universiteit Leiden, Leiden, the Netherlands.

Oyarzun, R., Arumi, J., Salgado, L., Marino, M., 2007. Sensitivity analysis and field testing of RISK-N model in the Central Valley of Chile. Agricultural water management 87, 251–260.

Richards, K., Coxon, C.E., Ryan, M., 2005. Unsaturated zone travel time to groundwater on a vulnerable site. Irish Geography 38, 57–71.

Ryan, M., Fanning, A., 1996. Effects of fertilizer N and slurry on nitrate leaching – lysimeter studies on 5 soils. Irish Geography 29, 126–136.

SAS, 2003. SAS for Windows. Version 9.1. SAS Inst, Cary, NC.

Schulte, R.P.O., Diamond, J., Finkele, K., Holden, N.M., Brereton, A.J., 2005. Predicting the soil moisture conditions of Irish grasslands. Irish Journal of Agricultural and Food Research 44, 95–110.

Swartz, M., Misstear, B.D.R., Farrell, E.R., Daly, D., Deakin, J., 1999. The Role of Subsoil Permeability in Groundwater Vulnerability Assessment. XXIX IAH Congress 1999. IAH, Bratislava, Slovac Republic.

Tobin, J., 1958. Estimation of relationship for limited dependent variable. Econometrica 26, 24–36.

Vellidis, G., Hubbard, R.K., Davis, J.G., Lowrance, R.G., Williams, R.G., Johnson Jr., J.C., Newton, G.L., 1996. Nutrient concentration in the soil solution and shallow ground water of a liquid dairy manure land application site. Transactions of the ASAE 39.

Yidana, S.M., Ophori, D., Banoeng-Yakubo, B., 2008. Hydrochemical evaluation of the Voltaian system – the Afram Plains area, Ghana. Journal of Environmental Management 88, 697–707.